Biorheology 39 (2002) 419–424
IOS Press

Quantification of the non-planarity of the human carotid bifurcation

E. King [a], X.Y. Xu [b], A.D. Hughes [c], Q. Long [b], S.A. Thom [c] and K.H. Parker [d,*]

[a] *Department of Physics, Imperial College of Science, Technology & Medicine, London, UK*

[b] *Department of Chemical Engineering, Imperial College of Science, Technology & Medicine, London, UK*

[c] *Department of Clinical Pharmacology and Therapeutics, Imperial College of Science, Technology & Medicine, London, UK*

[d] *Department of Bioengineering, Imperial College of Science, Technology & Medicine, London, UK*

Abstract. The carotid bifurcation has been a region of particular interest due to its predilection for clinically significant atherosclerosis. It has been shown that the vessel geometry is a major determinant of the local haemodynamic properties which are believed to be associated with the location of atherosclerotic lesions. Current knowledge of the geometry of the carotid bifurcation is insufficient and restricted to basic geometric parameters. To provide some means of quantifying the degree of complexity of the 3D shape of the bifurcation, we made an initial attempt by evaluating the non-planarity of an arterial bifurcation based upon the singular value decomposition theorem.

In this paper we present our results obtained on the right carotid bifurcations of six normal subjects, each of whom was scanned twice using the 2D time-of-flight MR sequence. The acquired 2D cross sectional images were processed by using our in-house software which comprises 2D segmentation, 3D reconstruction and smoothing. The centroids of each transverse slices were determined and used as input data for the non-planarity analysis. Our results using the singular value decomposition method have demonstrated discernible differences in non-planarity among individuals. Comparisons with the planarity definition proposed by other investigators suggest that the singular value decomposition method offers more information about the linearity and planarity of the bifurcation. However, it is also realised that a single measure of non-planarity can never fully characterise a bifurcation owing to the great variety of geometries.

Keywords: MRI, carotid bifurcation, singular value decomposition, non-planarity

1. Introduction

It is now generally accepted that the genesis and distribution of arterial disease is influenced by local haemodynamic factors. Support for this derives from studies of the focal distribution of disease in humans [2,5,8], correlations between the distribution of early lesions in experimental animals and haemodynamic measurements in casts of the experimental vessels [9]. More recently, *in vitro* studies on endothelial cultures have shown that virtually every function of the cells is altered by the degree of fluid movement in the culture medium [1,8].

There is also a growing belief that subtle variations in the anatomical shape of arteries can have significant influence on local haemodynamics. Our current knowledge of the geometry of an arterial bifurcation is insufficient and restricted to basic geometric parameters, such as the diameters of its main branches and the angles between them. To advance the discussion beyond the anecdotal and to provide a basis for

*Address for correspondence: Dr. K.H. Parker, Department of Biomedical Engineering, Imperial College of Science, Technology and Medicine, London SW7 2BY, UK. Tel.: +44 207 594 5171; Fax: +44 207 594 5177; E-mail: k.parker@ic.ac.uk.

testing this hypothesis, we believe that it will be necessary to develop some means of quantifying the degree of complexity of the the shape of an artery. Realising the fact that the three main vessels at an arterial bifurcation are unlikely to lie in the same plane, and the potential importance of non-planarity as a geometric variable influencing the local flow patterns, we made an initial attempt by evaluating the non-planarity of an arterial bifurcation based upon the singular value decomposition theorem.

In this paper we will present the outline of the method and apply it to the analysis of carotid bifurcations of a number of subjects measured using magnetic resonance imaging (MRI). For the cases shown, we analyse the skeleton of the bifurcation determined by 3D image analysis techniques from sequential transverse images of the bifurcation. The method, however, is not reliant upon this skeletonisation and would work equally well on, for example, a description of the bifurcation as either a structured or unstructured cloud of ‘wall’ points [1].

2. Theory

The singular value decomposition theorem states that any $(n \times m)$ matrix $\mathbf{X}$ can be written in the ‘nearly’ unique form [6]

$$\mathbf{X} = \mathbf{UWV^T},$$

where:

$\mathbf{U}$ is an $(n \times m)$ matrix,
$\mathbf{V}$ is an $(m \times m)$ basis matrix,
$\mathbf{U}$ and $\mathbf{V}$ are orthonormal with $\mathbf{U^TU} = \mathbf{V^TV} = \mathbf{I}$,
$\mathbf{W}$ is an $(m \times m)$ diagonal matrix with non-negative elements with $W_{11} \geqslant W_{22} \geqslant W_{33} \ldots$ (the singular values). For our data, $m = 3$ and n is the number of points describing the vessels.

Practically, the first row of the basis matrix $\mathbf{V}$ is a unit vector defining the line of best fit to the data $\mathbf{X}$ in the least-squares sense, the first column of $\mathbf{U}$ is the projection of $\mathbf{X}$ onto this line and the first singular value W_{11} is a measure of the ‘amount’ of the data that can be ‘explained’ by this single line.

Similarly, the first two rows of $\mathbf{V}$ define the plane of best fit to the data, the first two columns of $\mathbf{U}$ are the projection of $\mathbf{X}$ onto this plane and W_{22} is a measure of the amount of the data that is explained by going from a 1D to a 2D representation of the data.

In this paper, we consider a set of n points describing a 3D object, the carotid bifurcation; either points lying in the vessel walls or points describing the skeleton of the vessels. (X) is an $(n \times 3)$ matrix where each row is the vector describing the position of an individual point in an arbitrary frame of reference. In this case, $\mathbf{U}$ is a complete description of the data in the coordinates given by $\mathbf{V}$ and W_{33} is a measure of the amount of the data which is explained by going from the 2D to a 3D representation of the data. If $\mathbf{X}$ is dimensional, then $\mathbf{W}$ is dimensional and cannot be used directly as a frame-indifferent measure of geometry. However, the trace of the the matrix, $Tr(\mathbf{W}) = \sum_i W_{ii}$, is a measure of $\mathbf{X}$. We therefore propose the scaled singular values $S_n = W_{nn}/Tr(\mathbf{W})$ as measures of non-planarity of the data $\mathbf{X}$.

S_1 indicates the fraction of the data that can be ‘represented’ on a single line. S_1 and S_2 together indicate the fraction of the data that can be represented on a plane. Since, by definition, $\sum_i S_i = 1$, S_3 is a measure of the fraction of the data that is non-planar. We note that since $W_{11} \geqslant W_{22} \geqslant W_{33}$, $0 \leqslant S_3 \leqslant 1/3$.

The meaning of the scaled singular values can, perhaps, be best illustrated by indicating the results that would be obtained for a variety of idealised geometries. For a homogenous set of points describing a sphere, there is no preferred direction and we would obtain $S_1 = S_2 = S_3 = 1/3$. For a circular cylinder whose length is larger than its radius, we would obtain $S_1 > S_2 = S_3$ where the magnitude of the inequality would be determined by the aspect ratio of the cylinder. For a segment of a torus, we would obtain $S_1 > S_2 > S_3$ where the magnitude of the second inequality would indicate the degree of curvature of the segment in the plane of the torus to its radius. For a circular cylinder following a helical path, we would again obtain $S_1 > S_2 = S_3$ where the magnitude of S_2 and S_3 would reflect both the radius of the cylinder and the radius of the helix. If the set of points lie in a 3D surface, as in all of the previous examples, then $s_3 \neq 0$. If we consider a linear representation of a 3D object, such as the skeleton used in the examples below, then it is possible for $S_3 = 0$. Thus, for the skeleton of a straight, circular cylinder we would obtain $S_1 = 1, S_2 = S_3 = 0$; for the skeleton of a segment of a torus, $S_3 = 0$; but for the skeleton of a helical circular cylinder, $S_3 \neq 0$ because the skeleton would no longer lie within a plane.

We also note that the singular value decompostion of the data provides an easy means of displaying the best fit coordinates and its projection onto the best fit plane.

3. Methods

The anatomical data used to test the algorithm was derived from young, healthy, male subjects as part of a reproducibility study in which each subject was scanned on two separate occasions. The methods of imaging and image processing used to produce the images of the lumen of the carotid bifurcation and their skeletons has previously been described in detail [4]. Briefly, an axis roughly parallel to the right common carotid artery was determined, the z-axis, and a 2D time-of-flight MR sequence was used to obtain cross sectional images transverse to this axis. A total of 60 slices, 1.5 mm apart were obtained. The 2D cross sectional images were segmented by using an active contour method, and the centroids of all cross sections were determined. After 3D geometry reconstruction and smoothing, new centroids at equally spaced cross sections were determined. The data were interpolated to give points 0.1 mm apart along the z-axis, 500 points for the common carotid and 400 points each for the internal and external carotid arteries.

4. Results

The results of the application of the singular value decomposition algorithm to a carotid bifurcation are shown in Fig. 1. Figure 1(a) shows the surface rendered vessels determined from the MRI scans, 1(b) orthogonal views of the skeleton of the bifurcation in and normal to the best-fit plane, and 1(c) a scaled 3D view of the skeleton and its projection onto the best-fit plane where the scaling factors for each axis are the corresponding singular values.

Figure 2 shows the three scaled singular values, S_1, S_2 and S_3 determined for six subjects. Note that for all of the subjects, S_1 is approximately 80% and S_2 10–15%. Thus, the non-planarity for all of the bifurcations is relatively small but still potentially important.

The proposed measure of non-planarity, S_3, is shown again in Fig. 3 (upward triangles) which also includes the values calculated from the second scan of each subject in this reproducibility study (downward triangles). We see that the reproducibility of the scans and subsequent analysis is reasonable good

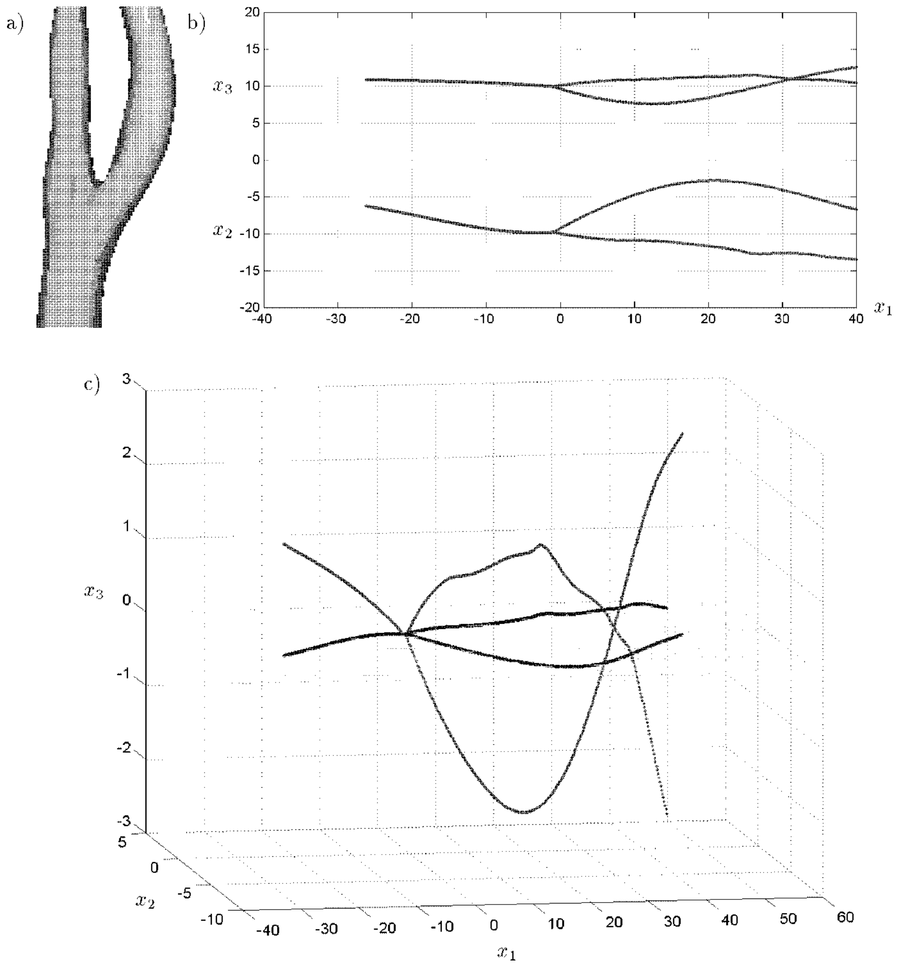

Fig. 1. The right carotid arterial bifurcation of one the six subjects studied. (a) The surface rendered vessels determined from MR scans. (b) Orthogonal views of the skeleton of the bifurcation in (top) and normal to (bottom) the best-fit plane where the axes are in units of the distance between sample points (0.1 mm). (c) A 3D representation of the skeleton and its projection onto the best-fit plane where the axes are scaled by their corresponding singular values. The best-fit plane is determined from the singular value decomposition (the rows of **V**) and the values in the x_3 direction represents the deviation of the skeleton from the planar.

($<1\%$). We also see that there is a measurable difference between S_3 for different subjects, although subjects 3–6 display very similar values.

It is obvious that the results of the analysis will depend upon the length of the vessels included in the analysis. In this study we have included 5 cm of the common carotid artery and 4 cm of the internal and external carotid arteries. This choice is somewhat arbitrary and dependent upon the properties and resolution of the MR scanner. It was also influenced by another part of the study which was the comparison of MR and 3D ultrasound scans which forced us to take into account the accessibility of the carotid arteries to ultrasound scanning. As a test of the influence of this factor in the calculation of S_3, we repeated the analysis for a variable number of points for one of the bifurcations. Figure 4 shows the three scaled singular values as a function of the number of points, outward from the point of bifurcation, included in the analysis. For the interpolated data used in this study, each point represents 0.1 mm.

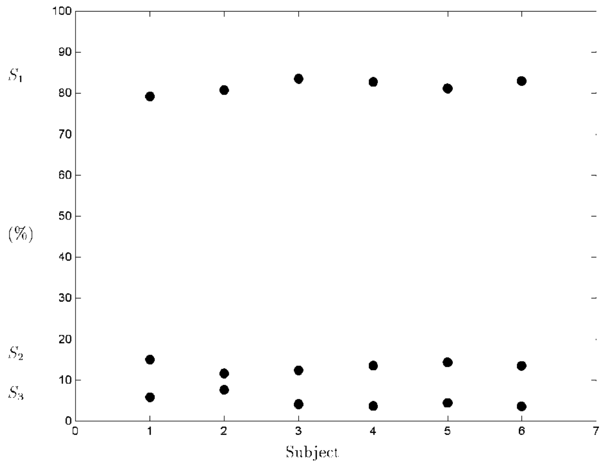

Fig. 2. The scaled singular values, S_1, S_2 and S_3 for the skeletons of the carotid bifurcation for the 6 subjects. S_1 indicates the percentage of the data that can be represented on a best-fit line, S_1 and S_2 indicate the percentage of the data that can be represented on a best-fit plane and S_3 indicates the percentage of the data that is non-planar.

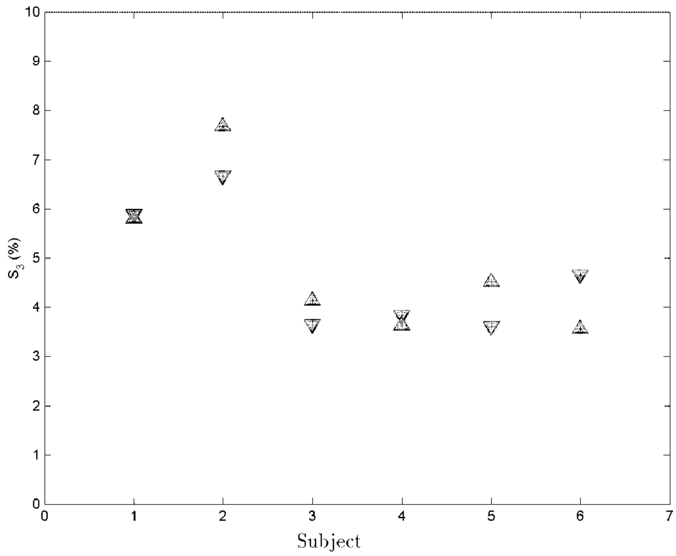

Fig. 3. In order to check the reproducibility of the anatomical measurements, all 6 subject were scanned twice. This plot shows S_3 for both scans with the upward triangle corresponding to the scan shown in Figs 1 and 2.

Finally, from our experience in applying this algorithm to anatomical data, we realise that a single measure of non-planarity can never fully characterise a bifurcation as the variety of geometries is too great. However, we have found the singular value decomposition of the data to be easy to apply and very informative. The identification of the best-fit plane for the bifurcation provides a very convenient frame of reference for comparing bifurcations. It also provides a means for more sophisticated analysis of the geometry of a bifurcation such as moments of distances away from the best-fit plane which may be necessary for a more complete description of a bifurcation.

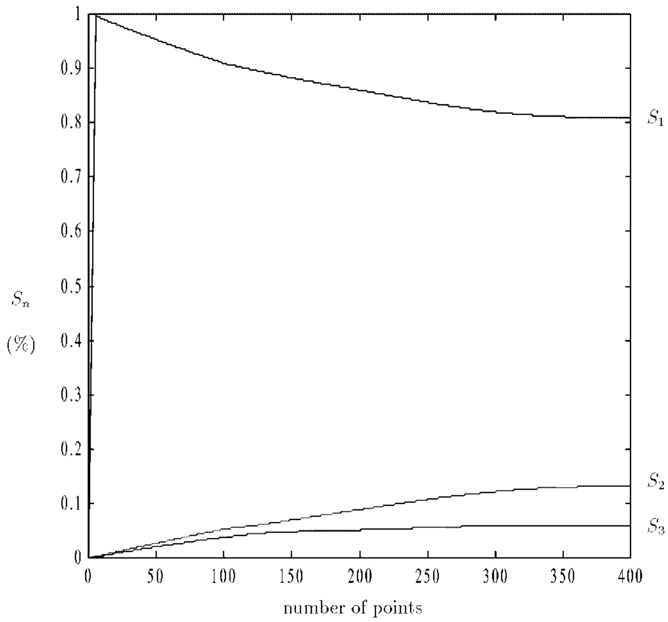

Fig. 4. The scaled singular values, S_1, S_2 and S_3 for one bifurcation as a function of the number of points per artery included in the analysis. Each point corresponds to 0.1 mm.

References

[1] K. Affeld, L. Goubergrits, J. Fernandez-Britto and L. Falcon, Variability of the geometry of the human common carotid artery. A vessel cast study of 31 specimens, *Pathol. Res. Pract.* **194** (1998), 597–602.
[2] C.G. Caro, J.M. Fitz-Gerald and R.C. Schroter, Arterial wall shear and distribution of early atheroma in man, *Nature* **223** (1969), 1159–1161.
[3] P.F. Davies, Flow-mediated endothelial mechanotransduction, *Physiol. Rev.* **75** (1995), 519–560.
[4] Q. Long, X.Y. Xu, M.W. Collins, M. Bourne and T.M. Griffith, Magnetic resonance image processing and structured grid generation of a human abdominal bifurcation, *Comput. Meth. Prog. Bio.* **56** (1998), 249–259.
[5] J.R.A. Mitchell and C.J. Schwartz, *Arterial Disease*, Blackwell Scientific Publications, Oxford, 1965.
[6] W.H. Press, B.P. Flannery, S.A. Teukolsky and W.T. Vetterling, *Numerical Recipies in C*, Cambridge University Press, Cambridge, 1988, pp. 60–72.
[7] J.Y.-J. Shyy, Y.-S. Li, M.-C. Lin, W. Chen, S. Yuan, S. Usami and S. Chien, Multiple cis-elements mediate shear stress-induced gene expression, *J. Biomech.* **28** (1995), 1451–1457.
[8] P.D. Weinberg, Disease patterns at branches and their relation to flow, *Biorheology* **39** (2001), 433–437.
[9] C.K. Zarins, D.P. Giddens, B.K. Bharadvaj, V.S. Sottiurai, R.F. Mabon and S. Glagov, Carotid bifurcation atherosclerosis: Quantitative correlation of plaque localization with flow velocity profiles and wall shear stress, *Circ. Res.* **53** (1983), 502–514.